

Hadron cross sections at ultrahigh energies and unitarity bounds on diffraction

T. K. Gaisser

Bartol Research Foundation of the Franklin Institute, University of Delaware, Newark, Delaware 19716

U. P. Sukhatme

Department of Physics, University of Illinois at Chicago, Chicago, Illinois 60680

G. B. Yodh

Department of Physics and Astronomy, University of Maryland, College Park, Maryland 20742

(Received 19 June 1986)

The proton-air inelastic cross section, obtained from cosmic-ray data at $\sqrt{s} = 30$ TeV, is compared with calculations using various different models for the energy variation of the parameters of the elementary proton-proton interaction. Three conclusions are derived. (1) The diffractive dissociation cross section for proton-air interactions is determined with an uncertainty of less than three percent because unitarity bounds the diffractive cross section from above. (2) Current models in which the proton-proton total cross section has an energy dependence of the form $c + d \ln^2(s)$ are favored by cosmic-ray data. (3) The proton-proton total cross section at $\sqrt{s} = 30$ TeV should be ≥ 130 mb, if the elastic slope parameter is less than 30 GeV^{-2} . If the Chou-Yang relationship between the slope parameter B and σ_{tot} is used, the Fly's Eye limits suggest that $\sigma_{\text{tot}} = 175^{+40}_{-27}$ mb.

I. INTRODUCTION

The behavior of total cross sections at ultrahigh energies ($\sqrt{s} > 1$ TeV) has been derived from analysis of air-shower observations.¹ The proton-air inelastic cross section determined from cosmic-ray data must be related to the basic proton-proton interaction to determine which of the different models for the ultrahigh-energy behavior of the scattering amplitude are consistent with cosmic-ray data and which can be ruled out. The adjective "inelastic" for the proton-air cross section $\sigma_{p\text{-air}}^{\text{inel}}$ describes the fact that cosmic-ray experiments do not measure all of the absorptive cross section because cascade development is not sensitive to processes that lead to quasielastic excitation of the air nucleus σ_{qe} , or to diffractive excitation of one of the nucleons of the air nucleus, σ^* . The method generally used² to calculate the p -air inelastic cross section from proton-proton parameters is the Glauber multiple-scattering technique. The application of this method leads to the relation

$$\sigma_{p\text{-air}}^{\text{inel}} = \sigma_{p\text{-air}}^{\text{tot}} - \sigma_{p\text{-air}}^{\text{el}} - \sigma_{\text{qe}} - \sigma^* - \Delta\sigma(\text{inelastic screening}). \quad (1.1)$$

The term $\Delta\sigma(\text{inelastic screening})$ accounts for screening due to multiple scattering with excited nucleon intermediate states. To calculate the right-hand side of this relation it is necessary to know the values of σ_{tot}^{pp} , the forward elastic slope parameter $B^{pp}(t=0)$, the ratio of the forward real and imaginary parts of the amplitude ρ , single and double diffractive cross sections σ_{SD}^{pp} and σ_{DD}^{pp} , the shape of $d^2\sigma/dt dM^2$ at t_{min} for the diffractive process, $p + p \rightarrow p + X$, and the nuclear density.²

In Sec. II, we summarize the basic features of the models used to describe the behavior of high-energy ele-

mentary pp and $\bar{p}p$ interactions. In Sec. III we state the basic equation for unitarity bounds on diffractive cross sections and show that any model which ascribes the increase in pp and $\bar{p}p$ cross sections entirely to diffractive processes will violate this bound at some energy. We show that the uncertainties in previous calculations^{1,2} using Eq. (1.1) can be further reduced by recognizing that the correction term σ^* must be bounded by unitarity. In the final section we present graphs showing contours of constant proton-air inelastic cross section as a function of σ_{tot}^{pp} and $B^{pp}(t=0)$ which can be used to derive the values of σ_{tot}^{pp} and B^{pp} allowed by the measured value of p -air inelastic cross section from cosmic-ray air-shower experiments. We show that models with a $\ln^2(s)$ increase in σ and B are favored. The basic multiple-scattering formalism is reviewed in an Appendix.

II. MODELS OF THE ELEMENTARY HADRON-HADRON INTERACTION

Many different models for the high-energy behavior of scattering amplitudes have been proposed.^{3,4} They may be roughly classified into four types: (1) geometrical-scaling models,⁵ (2) diffraction-dominance models,⁶ (3) factorized eikonal- (Chou-Yang-) type models,⁷ and (4) Reggeon-field-theory models.⁸

Geometrical-scaling models are based on the observation that the elastic differential cross section $d\sigma/dt$ vs t is similar to a classical diffraction pattern in optics. Indeed, if one takes the interaction radius R to be an increasing function of \sqrt{s} , then one expects all cross sections to rise like $R^2(\sqrt{s})$ and the first dip location $|t_{\text{dip}}|$ to move to smaller values. The key feature of the geometrical-scaling approach is the assumption that the entire energy dependence comes from just one source

$R(\sqrt{s})$, which has the dimensions of length. An immediate consequence is the prediction of a scaling curve in the dimensionless quantity $R^{-4}(\sqrt{s})d\sigma/dt$ vs $tR^2(\sqrt{s})$. It has been known for many years that a geometrical-scaling curve works reasonably well over the CERN ISR energy range,⁵ especially when the real parts of the scattering amplitude are incorporated into the formalism using derivative analyticity relations.⁹ Unfortunately, geometrical-scaling models run into trouble when they are confronted with the recent CERN $S\bar{p}pS$ collider data, since they predict the ratio of σ_{el}/σ_{tot} to remain constant with energy.³

The diffractive-dominance models ascribe all the rise in total cross sections to σ_{el} , σ_{SD} , and σ_{DD} , the inelastic cross section remaining constant.⁶ The ratio $\sigma_{inel}/\sigma_{tot}$ decreases with energy; σ_{el}/σ_{tot} becomes energy independent; σ_{SD}/σ_{tot} slowly decreases with energy while σ_{DD}/σ_{tot} will be asymptotically constant. We shall show in the next section that such a model violates unitarity bounds on diffraction dissociation. Furthermore, there is now preliminary experimental evidence that the rise in σ_{tot} is related to inelastic events producing "mini-jets."¹⁰

In the factorized eikonal⁷ (Chou-Yang-) type models the ratio σ_{el}/σ_{tot} need not be constant with energy. However, the detailed behavior of σ_{tot} , σ_{SD} , or σ_{DD} is not generally prescribed. These models do provide a reasonably good description of $d\sigma/dt$ data up to $S\bar{p}pS$ collider energies when the total cross section is used as input.

In Reggeon field theory,⁸ one takes the Pomeron to be a pole in the angular momentum plane and computes corrections coming from multi-Pomeron cuts. Such a "perturbative Reggeon scheme" is phenomenologically successful provided the bare Pomeron intercept is taken above unity [at approximately $\alpha_p^0(0)=1.13$] (Ref. 11). Diffraction-dissociation effects come from unitarity cuts of enhanced diagrams. It is thought that successive excitation of heavy flavors may be the physical mechanism underlying the rise of σ_{tot} (Ref. 12). Diagrams involving Pomeron exchanges and triple-Pomeron interactions can be thought of as coming from an effective two-dimensional Reggeon field theory⁸ in which rapidity plays the role of time. The asymptotic behavior, corresponding to a Pomeron trajectory intercept equal to one, involves a phase transition characterized by several critical indices. The "critical Pomeron solution"¹³ does predict slowly rising total cross sections, $\sigma_{tot} \sim \ln^{0.28}(s)$, but is clearly in conflict with an increase of the ratio σ_{el}/σ_{tot} .

Thus it may seem at first glance that with so much freedom it would be possible to fit the cosmic-ray data with a large range of models. This is not so, however, because the range of variation of the diffractive component cross sections are limited by unitarity bounds. There is only one proviso for this statement, which is that Glauber techniques are valid at these high energies.

III. UNITARITY BOUNDS AND LIMITS ON DIFFRACTION

The unitarity bound on elastic and diffractive cross section can be stated as¹⁴

$$\sigma_{el} + \sigma_{diff} \leq \frac{1}{2}\sigma_{tot} \quad (3.1)$$

This constraint, which is most easily derived in impact-parameter space, follows from s -channel unitarity and the usual requirement that diffraction is purely absorptive (shadow of nondiffractive particle production). More specifically, the scattering submatrix for diffractive states is taken to be purely imaginary iG , and the eigenvalues of the real matrix G are required to lie in the range 0–1 (Ref. 14).

One can write σ_{tot} in terms of its parts

$$\sigma_{tot} = \sigma_{el} + \sigma_{diff} + \sigma_{ND} \quad (3.2)$$

where σ_{ND} is the nondiffractive cross section. It follows from these relations that

$$\sigma_{ND} \geq \frac{1}{2}\sigma_{tot} \quad (3.3)$$

which means that if $\sigma_{tot}(E)$ increases with energy then σ_{ND} cannot be energy independent.

Assuming the general validity of the bounds we apply it to the specific model of diffractive dominance proposed by Goulianos.⁶ The energy variations of σ_{el} , $2\sigma_{SD}$, σ_{DD} , and σ_{tot} for this model are shown in Fig. 1. The value of $\frac{1}{2}(\sigma_{tot})$ is also graphed. The unitarity bound given by Eq. (3.1) is violated by this model for $\sqrt{s} \geq 200$ GeV; so is the inequality $\sigma_{ND} \geq \frac{1}{2}(\sigma_{tot})$. In fact, any model which ascribes the increase in cross section entirely to diffractive processes will violate conventional unitarity requirements (see the Appendix and Gaisser *et al.*²).

As representative of other models let us consider the parametrization proposed by Block and Cahn.⁴ The model gives explicit fits for total and elastic cross sections as well as the slope parameter B , as a function of energy. To obtain σ_{p-air}^{inel} using Eq. (1.1) we must calculate the five terms on the right-hand side using Glauber methods. The total, elastic and quasielastic, proton-air cross sections can be calculated in a straightforward manner using model parameters: σ_{tot}^{pp} , σ_{el}^{pp} , B^{pp} , and ρ . To estimate σ^* and $\Delta\sigma$ (inelastic screening) a knowledge of the single-diffractive cross section is needed, which is not given by the model. Of these two terms, $\Delta\sigma$ (inelastic screening) depends only on the value of $d^2\sigma/dt dM^2$

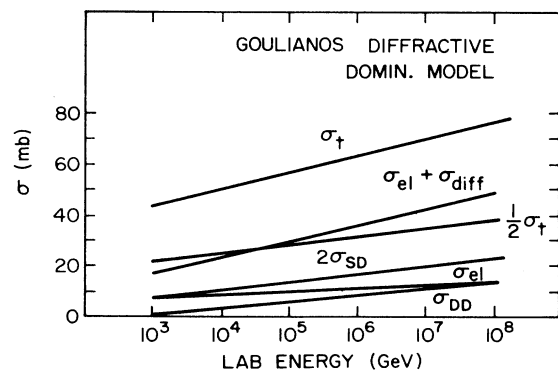


FIG. 1. Ultrahigh-energy predictions of pp cross sections using a diffractive dominance model [Goulianos (Ref. 6)]. This model clearly violates the unitarity bound $\sigma_{el} + \sigma_{diff} \leq \frac{1}{2}\sigma_{tot}$ for $E_{lab} \geq 2 \times 10^4$ GeV.

at t_{\min} which varies as $1/M^2$ (Ref. 2). Most of the contribution to this term comes from small values of M^2 and numerical evaluation gives a value for this correction which varies from about 8 mb at ISR energies to saturation at ~ 14 mb at ultrahigh energies (see Gaisser *et al.*²).

The correction for diffraction dissociation of the target nucleon is given by

$$\sigma^* = (\sigma_{SD}^{pp}/\sigma_{inel}^{pp})\sigma_{p-air}^1 \quad (3.4)$$

Here, σ_{p-air}^1 is the cross section for an absorptive p -nucleus interaction involving exactly one elementary inelastic encounter. It is easy to show that $\sigma_{p-air}^1 \equiv 2\pi\langle r^2 \rangle/3$ which corresponds to 142 mb for a root-mean-square radius of 2.6 F. The correction depends on the energy dependence of $\sigma_{SD}^{pp}/\sigma_{inel}^{pp}$ where $\sigma_{inel}^{pp} \equiv \sigma_{tot} - \sigma_{el} = \sigma_{ND} + 2\sigma_{SD} + \sigma_{DD}$.

What does the unitarity bound tell us about this ratio? The unitarity bound in Eq. (3.1) gives

$$2\sigma_{SD} + \sigma_{DD} \leq \frac{1}{2}\sigma_{tot} - \sigma_{el} \quad (3.5)$$

The maximum value of σ_{SD} is then obtained by putting $\sigma_{DD} = 0$. The ratio of $\sigma_{SD}/\sigma_{inel}$ is bounded by

$$\sigma_{SD}/\sigma_{inel} \leq \frac{1}{4} \left[1 - \frac{\sigma_{el}/\sigma_{tot}}{1 - \sigma_{el}/\sigma_{tot}} \right] \leq 0.25 \quad (3.6)$$

The maximum value of σ^* is 36 mb if $\sigma_{el} = 0$. In the Block-Cahn model with a $[\ln(s)]^2$ energy dependence,⁴ the ratio of σ_{el} to σ_{tot} varies from 0.175 to 0.37 as energy is varied from $\sqrt{s} \sim 20$ GeV to $\sqrt{s} \sim 10$ TeV. The corresponding upper limits on σ^* are 28 and 15 mb, respectively. At ISR energies, however, there are direct measurements of σ_{SD} and σ_{inel} which give a 14-mb cross section for σ^* . A reasonable measure of the allowed range of σ^* can be obtained by assuming that the lower bound to $\sigma_{SD}/\sigma_{inel}$ is the ISR value and the upper bound is given by Eq. (3.6) with σ_{el}/σ_{tot} being taken from Block-Cahn model. The result is shown in Fig. 2. Also shown in the figure is the sum of the last three terms in Eq. (1.1), i.e., $\sigma_{qe} + \sigma^* + \Delta\sigma$ (inelastic screening). The fractional uncertainty in the value of σ_{p-air}^{inel} is less than three percent.

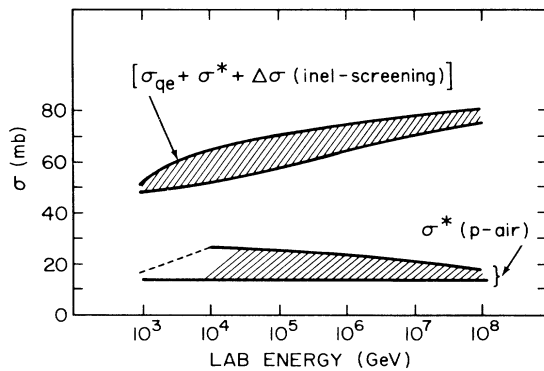


FIG. 2. Allowed ranges for the correction for diffractive dissociation of the target nucleon. Also shown is the total correction as a function of energy.

IV. ASYMPTOTIC CROSS SECTIONS FROM COSMIC-RAY DATA

First, we present the energy variation of proton-air inelastic cross sections as deduced by analysis of cosmic-ray experiments from 4×10^5 to 10^9 GeV (Refs. 15–17) in Fig. 3. One observes that the cross section is ~ 410 mb at 10^6 GeV and increases to between 550 and 600 mb at energies above 10^7 GeV.

Next, we display as an example, the energy variation of the parameters of the elementary pp interactions (σ_{tot} , σ_{el} , and B), needed as input to Glauber calculations, in Figs. 4(a), 4(b), and 4(c) according to the work of Block and Cahn.⁴ The cross-section graph [Fig. 4(a)] is identical to Fig. 16(a) of Ref. 4. The cross sections in Fig. 4(a) are found by fitting both the σ_{tot} and ρ for energies at or below ISR energies. The upper curve corresponds to an assumed energy dependence of the total cross section of $\ln^2(s/s_0)$, where s_0 is a scale constant fitted by the data. The lower curve assumed an energy dependence of σ_{tot} that behaves as $\ln^2(s/s_0)/[1 + a \ln^2(s/s_0)]$, where a is also fitted by the data, and has the consequence that it behaves essentially as $\ln^2(s/s_0)$ over the ISR energy range, but asymptotically goes to a constant cross section. The elastic cross section [Fig. 4(b)] is calculated from

$$\sigma_{el} = \sigma_{tot}^2 / 16\pi B,$$

an approximation that neglects ρ^2 compared to unity and neglects the t dependence of the slope parameter $B(t)$. The upper curve in Fig. 4(b) corresponds to using the upper curve of Fig. 4(a) and the upper curve of Fig. 4(c), both of which are fits to the data. The lower curve in Fig. 4(b) uses σ_{tot} from the lower curve of Fig. 4(a) and B from the lower curve of Fig. 4(c). The slope parameter [Fig. 4(c)] comes from a separate fit [M. M. Block (private communication)] to an assumed energy dependence $a + B \ln(s) + c \ln^2(s)$ for the upper curve. The lower curve for B which corresponds to $\sigma \rightarrow \text{const}$ asymptotically, was calculated [M.M. Block (private communication)] from

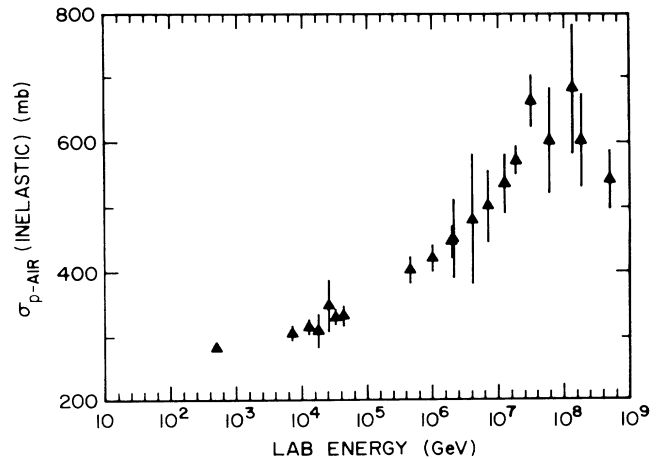


FIG. 3. The energy variation of σ_{p-air}^{inel} as determined from cosmic-ray experiments. The points above 10^6 GeV come from air-shower experiments; the energy bin widths for the points are not shown.

Fig. 9 of Ref. 4, which implicitly gives B as a function of σ_{tot} in the Chou-Yang model. The resulting Chou-Yang value of B vs \sqrt{s} gives an excellent reproduction of B in the ISR region and a good value of the $S\bar{p}pS$ point as well. The Chou-Yang model also reproduces the upper B vs \sqrt{s} curve in Fig. 4(c). This suggests that the Chou-Yang

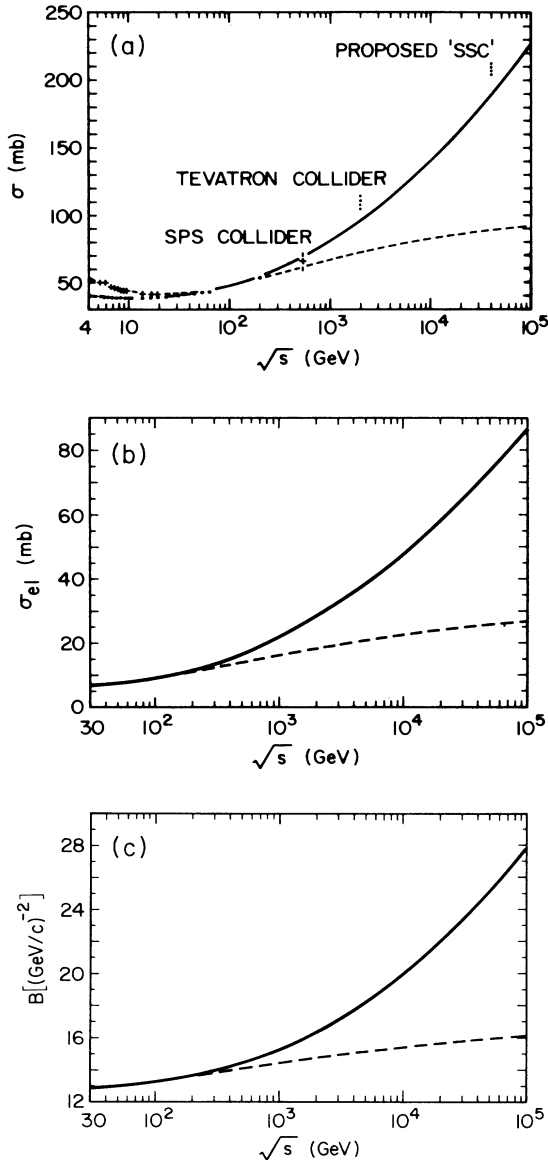


FIG. 4. (a) Energy variation of σ_{tot} for two models of Block and Cahn which fit both σ_{tot} and ρ for energies at or below the ISR energy. See text for details of the two fits. (b) Energy variation of σ_{el} for the same two models of Block and Cahn. The upper curve corresponds to using the upper curve of (a) and the upper curve of (c). The lower curve uses σ_{tot} from the lower curve of (a) and B from the lower curve of (c). (c) Energy variation of the elastic slope parameter for the models. The upper curve is a fit of B to the data using an assumed energy dependence $A + B \ln(s) + C \ln^2(s/s)$. The lower curve used the Chou-Yang relation between B and σ_{tot} , and gets the energy dependence by using the lower curve (asymptotically constant cross section case) of (a).

relation between B and σ_{tot} may be used reliably for extrapolation to high energies.

To determine what value of the pp total cross section is implied by cosmic-ray data in the energy range $\sqrt{s} \sim 6\text{--}20$ TeV (this corresponds to energies of primary cosmic-rays varying from 1.8×10^7 to 2×10^8 GeV) we calculated contours of constant $\sigma_{p\text{-air}}^{\text{inel}}$ for different inputs for $\sigma_{\text{tot}}^{\text{pp}}$ and B^{pp} for the case when σ^* is calculated corresponding to only a slight increase of $\sigma_{\text{SD}}/\sigma_{\text{inel}}$ over ISR values. These contour plots are shown in Fig. 5.

We point out two important features of the shape of these contours: For a fixed value of $\sigma_{p\text{-air}}^{\text{inel}}$, an increase in the slope parameter B leads to a decrease in the value of $\sigma_{\text{tot}}^{\text{pp}}$ required to keep p -air cross section fixed. Also, if the slope parameter is small the contours become horizontal.

Next, we examine what pp cross section is implied by the Utah measurement of 540 ± 45 mb at a $\sqrt{s} \sim 30$ TeV (Ref. 17). The Utah point is lower than the Akeno¹⁶ points, so a study of its implications ought to give an estimate for lowest allowed values for the pp cross section. For this purpose we superpose on the contours the energy variation of the point $(B^{\text{pp}}, \sigma_{\text{tot}}^{\text{pp}})$ for two different models of Block and Cahn.⁴ The six points for each of the two models correspond to laboratory energies from 10^3 to 10^8 GeV in steps of factors of 10. These are the connected lines in Fig. 6. The highest-energy point of Block-Cahn model number 2 (with an asymptotically constant cross section) is only at 375 mb which is at least 3σ away from the cosmic-ray value.¹⁸ These qualitative features follow from the fact that the p -nucleon cross section saturates for large values of the p -nucleon cross section because shadowing becomes complete. The asymptotic size of the p -air cross section is then given by the convolution of the nuclear size and the size of the individual nucleons. The latter is given by the Fourier transform of the scattering amplitude, which is proportional to $\exp(-Bq^2/2)$. Therefore the saturation cross section is proportional to $a^2 + \text{const} \times (B)$.

The final result may be better presented using a set of

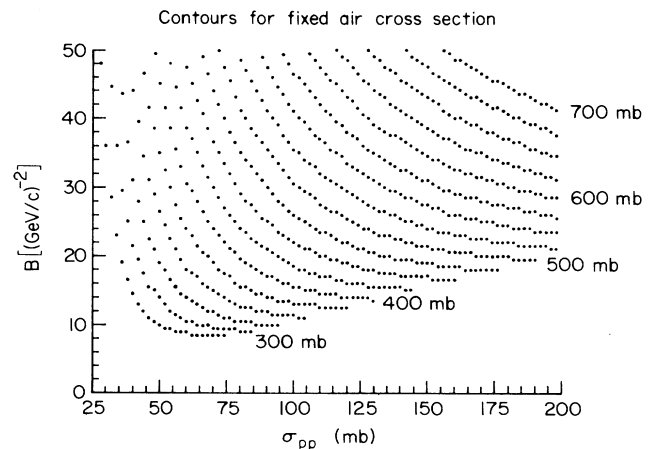


FIG. 5. Contour plots for the variation of the slope parameter B (y axis) with $\sigma_{\text{tot}}^{\text{pp}}$, for fixed values of $\sigma_{p\text{-air}}^{\text{inel}}$. The lowest contour is for $\sigma_{p\text{-air}}^{\text{inel}} = 275$ mb and the increment in cross section per contour is 25 mb in this figure and Fig. 6.

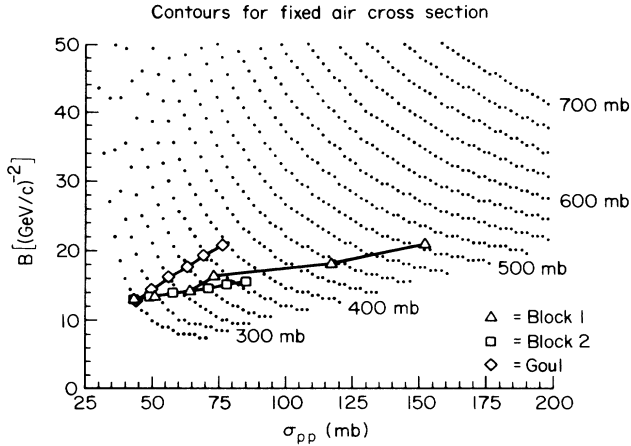


FIG. 6. In this figure we have superimposed the variation of B with σ_{tot}^{pp} as required by three models of the elementary interaction: Block and Cahn 1 and 2 and that of Goulianos. Only Block and Cahn model 1 reaches close to the Fly's Eye contour for 540 ± 45 mb.

contours of $\sigma_{p\text{-air}}^{\text{inel}}$ vs σ_{tot}^{pp} for fixed values of the slope parameter. This is shown in Fig. 7. Without discussing any particular model one can examine the implication of the Fly's Eye point. One can draw the conclusion that if $B = 40 \text{ GeV}^{-2}$, a $\sigma_{\text{tot}}^{pp} \sim 80 \text{ mb}$ at $\sqrt{s} \sim 30 \text{ TeV}$ could fit the cosmic-ray data at the 1σ level. However, fits to B and σ_{pp} must be made simultaneously. Using the fits of Ref. 4, one sees that a small value of σ_{pp} is correlated with a small value of B ($\sim 15\text{--}16 \text{ GeV}^{-2}$ at $\sqrt{s} \sim 30 \text{ TeV}$), which is inconsistent with the measured $\sigma_{p\text{-air}}^{\text{inel}}$ in Fig. 7. A more consistent value is $B \sim 25 \text{ GeV}^{-2}$ for which $\sigma_{\text{tot}}^{pp} \geq 130 \text{ mb}$.

The Chou-Yang relation between B and σ_{tot} referred to above can be used to remove the ambiguity from Fig. 7. This leads to the diagonal broken line on the figure. If this relation is used the Fly's Eye limits suggest

$$\sigma_{\text{tot}} = 175_{-27}^{+40} \text{ mb}$$

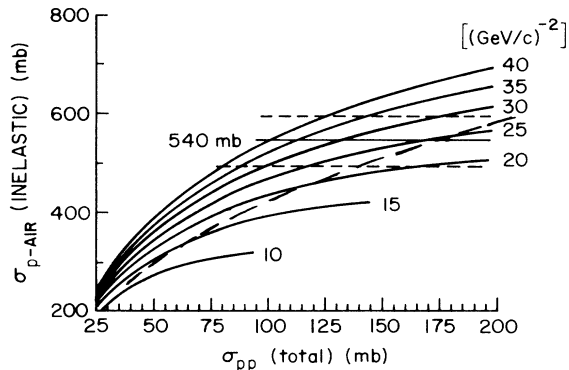


FIG. 7. The figure shows contours describing the variation of $\sigma_{p\text{-air}}^{\text{inel}}$ with σ_{tot}^{pp} for fixed values of the elastic slope parameter. The Fly's Eye cross section with its 1σ error band is shown. See text for discussion.

at $\sqrt{s} \sim 40 \text{ TeV}$. We conclude with a reminder that the air-shower measurements of $\sigma_{p\text{-air}}^{\text{inel}}$ above 10^{15} eV are not direct. They rely on a model-dependent analysis of the data.^{16,17,19} In particular, the conclusion about the cross section depends on assumptions made about fluctuations in individual hadronic interactions²⁰ and on the chemical composition of the primaries. We do not expect changes in hadronic interactions above 10^{15} eV to lead to large uncertainties in the inferred cross section.²¹ As concerns composition, the strategy adopted in Refs. 16 and 17 is to minimize this source of uncertainty by looking only at the most deeply penetrating showers, which are presumed to be initiated by protons rather than by heavier nuclei. Overall fluctuations in penetration for all showers are also sensitive to the cross section; however, they are more sensitive to uncertainty in the composition because there is no selection against contributions from heavy primaries. Comparison between overall fluctuations as summarized by Linsley²² and a calculation of fluctuations in depth of maximum for all showers,²⁰ leads us to the conclusion that this type of measurement cannot distinguish between a $\ln(s)$ or a $\ln^2(s)$ extrapolation of the cross section.¹ The data of Refs. 16 and 17 appear to favor the more rapid increase. All data are inconsistent with a cross section that does not increase significantly above the value measured at the $\bar{p}p$ collider.

ACKNOWLEDGMENTS

We are particularly grateful to Martin Block for many useful discussions. We also gratefully acknowledge the contribution of C. J. Noble to early phases of this work. This work was supported in part by the National Science Foundation and the Department of Energy.

APPENDIX

We collect here the basic formulas of the Glauber model²³ for relating nucleon-nucleon to nucleon-nucleus scattering so that the reader may judge their applicability to high-energy scattering. The amplitude for elastic scattering on a nucleus is

$$F(\mathbf{q}) = \frac{ik}{2\pi} \theta(q^2) \int d^2b e^{i\mathbf{q}\cdot\mathbf{b}} \int \cdots \int (\mathbf{b}, \mathbf{s}_1 \cdots \mathbf{s}_A) \times \prod_{i=1}^A \rho(\mathbf{r}_i) d^3r_i. \quad (\text{A1})$$

The profile factor Γ is related to the phase shift χ for the scattering by $\Gamma = 1 - e^{i\chi}$. The essential assumption of the Glauber model is that the overall phase shifts for the scattering on a nuclear target are the sum of the phase shifts for scattering on the individual nucleons:

$$\exp[i\chi(\mathbf{b})] = \prod_{j=1}^A \exp[i\chi_j(\mathbf{b}\cdot\mathbf{s}_j)]. \quad (\text{A2})$$

If we define a nucleon-nucleon profile

$$\Gamma_j = 1 - e^{i\chi_j} = \frac{1}{2\pi ik} \int e^{-i\mathbf{q}\cdot\mathbf{b}} f(\mathbf{q}) d^2q, \quad (\text{A3})$$

then Eq. (A1) becomes

$$F(q) = \frac{ik}{2\pi} \theta(q^2) \times \int d^2b e^{iq \cdot b} \left[1 - \left(1 - \int \Gamma_j(\mathbf{b}-\mathbf{s}) \times \rho(\mathbf{r}) d^3r \right)^A \right]. \quad (\text{A4})$$

The momentum transfer $\mathbf{q} = \mathbf{k} - \mathbf{k}'$, $\theta(q^2)$ is a recoil factor, \mathbf{k} and \mathbf{k}' are, respectively, the incident and final momentum of the nucleon, \mathbf{b} is the impact parameter in the plane normal to the collision axis, and \mathbf{s}_j is the projection of the position of the j th nucleon in that plane. $\rho(r_i)$ is the single nucleon density function, normalized to unity and $f(\mathbf{q})$ is the nucleon-nucleon scattering amplitude. The conventional form used to fit the elastic nucleon-nucleon amplitude at small angles is

$$f(q) = \frac{k\sigma_{\text{tot}}}{4\pi} (\rho + i) e^{-Bq^2/2}, \quad (\text{A5})$$

where ρ here is the ratio of the real to the imaginary part of the scattering amplitude.

A model for the nucleon-nucleon amplitude is inserted into Eq. (A4) to compute $F(\mathbf{q})$. Then the total cross section and the elastic cross section are obtained from

$$\sigma_{p\text{-air}}^{\text{tot}} = \frac{4\pi}{k} \text{Im}F(0), \quad (\text{A6})$$

and

$$\sigma_{p\text{-air}}^{\text{el}} = \int |F(\mathbf{q})|^2 d\Omega_{\mathbf{q}}. \quad (\text{A7})$$

The total and elastic cross sections were computed for a variety of nuclear targets using harmonic-oscillator forms for the density of nucleons in light nuclei, a Gaussian form for air, and the Woods-Saxon form for heavy nuclei. The three corrections in Eq. (1.1), σ^* , σ_{qe} , and $\Delta\sigma$ (inelastic screening), were computed using Gaussian density distributions.

The derivation of σ^* has already been discussed in the main text. The result for σ_{qe} is obtained from the work of Glauber and Matthiae²³ by integrating their expression for the contribution of quasielastic scattering to the differential cross section. For a Gaussian form of the nuclear density and $f(q)$ given by Eq. (A5),

$$\sigma_{\text{qe}} = \pi R^2 \sum_{n=1}^{\infty} \frac{\epsilon^n}{n}, \quad (\text{A8})$$

where

$$\epsilon \equiv \frac{1+\rho^2}{16\pi} \frac{\sigma_{\text{tot}}}{B}, \quad R^2 = \frac{2}{3} \langle a^2 \rangle,$$

and a is the rms nuclear radius. For air $\pi R^2 \approx 142$ mb. In a geometrical-scaling model $\sigma_{\text{tot}}/B = \text{const}$ with a value in the ISR range that gives $\epsilon \approx 0.17$. In fact, geometrical scaling is not valid up to $S\bar{p}pS$ collider energies, and ϵ increases slowly from 0.16 to 0.22 as σ_{tot} increases from 40 to 60 mb. Extrapolation (using Fig. 9 of Ref. 4) gives 0.31 when $\sigma_{\text{tot}} = 100$ mb. With these values of ϵ , σ_{qe} from Eq. (A8) is, respectively, 25, 35, and (extrapolating to $\sigma_{\text{tot}} = 100$ mb) 53 mb. The energy depen-

dence of σ_{qe} in this model thus depends on the energy dependence of σ_{tot} . The uncertainty in the extrapolation of ϵ contributes to the width of the bands in Fig. 2.

The inelastic-screening correction²⁴ is a correction to the Glauber calculation itself rather than a correction to the data. The multiple-scattering sum as written in Eq. (A4) contains only contributions from elastic nucleon-nucleon scattering. In addition, there are contributions in second- and higher-order diagrams from intermediate states in which the projectile nucleon is diffractively excited on one nucleon and reverts to its ground state in a later encounter. Including this correction to lowest order changes the integrand of Eqs. (A1) and (A4) to

$$\Gamma = 1 - (1 - \Gamma_i^{(0)})^A - \frac{A(A-1)}{2} (1 - \Gamma_i^{(0)})^{A-2} \sum_M \Gamma_M \Gamma_M^*, \quad (\text{A9})$$

where Γ_M is given in terms of $f_M(\mathbf{q})$ by an equation like (A3). The amplitude f_M for diffractive excitation to a mass M is given by²⁵

$$\frac{\pi}{k^2} \|f_M(q)\|^2 = \frac{d\sigma}{dM^2 dt} = A(M^2) e^{B(M^2)t}. \quad (\text{A10})$$

There is now a minimum longitudinal-momentum transfer $q_L = (M^2 - m^2)m/s$ needed to produce the mass $M > m$, so, in Eq. (A9),

$$\Gamma_M \rightarrow \int d^3r \rho(r) \frac{1}{2\pi i k} \int d^2q f_M(q) e^{-iq \cdot (b-s)} e^{iq_L z}, \quad (\text{A11})$$

where z is the component of \mathbf{r} normal to \mathbf{b} and \mathbf{s} is the component of \mathbf{r} in the plane of \mathbf{b} . Then, in the optical approximation [$B(M^2) \ll \langle a^2 \rangle$],

$$\sum_m \Gamma_M \Gamma_M^* \rightarrow 4\pi \int dM^2 A(M^2) \left| \int_{-\infty}^{\infty} \rho(b, z) e^{iq_L z} dz \right|^2. \quad (\text{A12})$$

Comparing Eqs. (A4) and (A9), and using the optical theorem, (A6), we find the correction to the cross section for the inelastic screening correction, which is given by an integral of the last term in Eq. (A9):

$$\Delta_{\text{inel}} = 4\pi \int d^2b \int dM^2 A(M^2) \times \exp\left[-\frac{1}{2}\sigma_{\text{tot}}T(b)\right] |F(q_l, b)|^2, \quad (\text{A13})$$

where

$$F(q_l, b) \equiv A \int_{-\infty}^{\infty} \rho(b, z) e^{iq_L z} dz.$$

(A here is the mass number of the target nucleus.) In obtaining (A13) the optical approximation has also been used for elastic scattering, assuming a purely imaginary elastic amplitude, so that

$$\Gamma_j(b) \rightarrow \frac{\sigma_{\text{tot}}}{2} \delta^2(\mathbf{b})$$

and

$$T(b) \equiv A \int_{-\infty}^{\infty} \rho(b, z) dz.$$

The large- A approximation has also been used, so that

$$\left[1 - \frac{Q}{A}\right]^A \rightarrow e^{-Q}.$$

Finally, to complete the estimate of the inelastic-screening correction, we take a Gaussian form for $\rho(r)$ and use the explicit fit of Ref. 25 for $A(M^2)$. The result is

$$\Delta\sigma_{\text{inel}}(\text{mb}) \approx \left[\frac{4\pi R}{\sigma_{\text{tot}}}\right]^2 [1 - (1+G)e^{-G}] \times \left[0.41 + 0.17 \ln \frac{E}{2m^2 R}\right], \quad (\text{A14})$$

where $G(A) \equiv A\sigma/2\pi R^2$, and R and $\sqrt{\sigma_{\text{tot}}}$ are in fermis. The relation

$$\sigma^{\text{abs}} = \sigma^{\text{tot}} - \sigma^{\text{el}} = \int d^2b [1 - |1 - \Gamma(b)|^2]$$

follows from Eqs. (A6) and (A7) and the definition of $f(q)$. From this relation and Eq. (A9) for $\Gamma(b)$ it is

straightforward to show that the inelastic screening correction to the absorptive cross section is

$$\Delta\sigma_{\text{inel}}^{\text{abs}}(A) \approx \frac{1}{4} \Delta\sigma_{\text{inel}}(2A).$$

For air $2A=29$, and the factor in square brackets in Eq. (A14) is nearly one. Thus the inelastic screening correction we have used in Eq. (1.1) is (for $R=2.12f$)

$$\Delta\sigma_{\text{inel}}^{\text{abs}} \approx \frac{5 \text{ mb}}{(\sigma_{40})^2} \left[1 + 0.4 \ln \frac{E}{20m_N}\right] \approx 10 \text{ mb},$$

where σ_{40} is σ_{pp}^{tot} in units of 40 mb.

To check the formalism for estimating the corrections to σ^{abs} we calculated² the cross sections of nucleons, pions, and kaons on a variety of nuclear targets and compared the results with accelerator data. For a range of targets and projectiles with beam energies from 10 to 1000 GeV, the calculated and observed values of $\sigma_{\text{hadron-}A}$ agree very well. We consider this to be an experimental test of the Glauber model and its corrections at ultrarelativistic energies.

- ¹G. B. Yodh, in *First Aspen Winter Physics Conference*, proceedings, Aspen, 1985, edited by M. M. Block (Ann. N. Y. Acad. Sci. **461**) (New York Academy of Sciences, New York, 1986), p. 239.
- ²V. Barger *et al.*, Phys. Rev. Lett. **33**, 1051 (1974); T. K. Gaisser *et al.*, in *Proceedings of the 14th International Cosmic Ray Conference, Munich*, edited by Klaus Pinkau (Max-Planck-Institut, München, 1975), p. 261; G. B. Yodh *et al.*, Phys. Rev. D **27**, 1183 (1983).
- ³Some recent reviews are U. Sukhatme, in *Multiparticle Dynamics 1985*, proceedings of the 16th International Symposium, Kiryat-Anavim, Israel, 1985, edited by J. Grunhaus (Editions Frontières, Gif-sur-Yvette, France, 1985); M. Giffon and E. Predazzi, Riv. Nuovo Cimento **7**, 1 (1984); N. Zotov, S. Rusakov, and V. Tsarev, Fix. Elem. Chastits At. Yadra **11**, 1160 (1980) [Sov. J. Part. Nucl. **11**, 462 (1980)].
- ⁴M. M. Block and R. Cahn, Rev. Mod. Phys. **57**, 563 (1985).
- ⁵J. Dias de Deus and P. Kroll, Acta Phys. Pol. B **9**, 159 (1978).
- ⁶K. Goulianos, Phys. Rep. **101**, 169 (1983), describes a specific model in which rising cross sections are attributed solely to diffraction. This paper also contains a summary of pp and $p\bar{p}$ data prior to 1983.
- ⁷T. Chou and C. N. Yang, in *Proceedings of Second International Conference on High Energy Physics and Nuclear Structure*, Rehovot, Israel, 1967, edited by G. Alexander (North-Holland, Amsterdam, 1967); F. Hayot and U. Sukhatme, Phys. Rev. D **10**, 2183 (1974); C. Bourrely, J. Soffer, and T. T. Wu, Phys. Rev. Lett. **54**, 757 (1985); H. Cheng, J. Walker, and T. T. Wu, Phys. Lett. **44B**, 97 (1973).
- ⁸V. N. Gribov, Zh. Eksp. Teor. Fiz. **56**, 892 (1969) [Sov. Phys. JETP **29**, 483 (1969)]; H. Abarbanel, J. Bronzan, R. Sugar, and A. White Phys. Rep. **21C**, 119 (1975); A. Migdal, A. Polyakov, and K. Ter-Martirosyan, Phys. Lett. **48B**, 239 (1974).
- ⁹J. Bronzan, G. Kane, and U. Sukhatme, Phys. Lett. **49B**, 272 (1974).
- ¹⁰UA1 Collaboration, F. Ceradin, in *Proceedings of the International Europhysics Conference on High Energy Physics*, Bari,

- Italy, 1985, edited by L. Nitti and G. Preparata (European Physical Society, Geneva, 1985).
- ¹¹A. Capella, J. Tran Thanh Van, and J. Kaplan, Nucl. Phys. **B97**, 493 (1975).
- ¹²T. K. Gaisser and Chung-I Tan, Phys. Rev. D **8**, 3881 (1973); J. Dash, S. Jones, and E. Manesis, *ibid.* **18**, 303 (1978); J. Dash and S. Jones, Z. Phys. C **22**, 49 (1984).
- ¹³A. White, in *Multiparticle Dynamics 1982*, proceedings of the XIII International Symposium, Volendam, The Netherlands, 1982, edited by W. Kittel, W. Metzger, and A. Stergiou (World Scientific, Singapore, 1983).
- ¹⁴J. Pumplin, Phys. Rev. D **8**, 2899 (1973); U. Sukhatme and F. Henyey, Nucl. Phys. **B108**, 317 (1976).
- ¹⁵M. Akashi *et al.*, Phys. Rev. D **24**, 2353 (1981). This paper contains the gamma family data from the Mt. Fuji emulsion-chamber experiment.
- ¹⁶T. Hara *et al.*, in *Proceedings of the International Symposium on Cosmic Rays and Particle Physics*, Tokyo, Japan, 1984, edited by A. Ohsawa and T. Yuda (Institute for Cosmic-Ray Research, Tokyo, 1984), p. 756; Phys. Rev. Lett. **50**, 2058 (1983). The 1984 paper gives the revised data points for the Akeno experiment.
- ¹⁷R. M. Baltrusaitis *et al.*, Phys. Rev. Lett. **52**, 1380 (1984). This paper contains results from the Fly's Eye experiment. The value quoted here is from R. M. Baltrusaitis *et al.*, in *Proceedings of the 19th International Conference on Cosmic Rays*, La Jolla, California, 1985, edited by F. C. Jones, J. Adams, and G. M. Mason (NASA Conf. Publ. 2376) (Goddard Space Flight Center, Greenbelt, MD, 1985), Vol. 6, p. 5, which is an updated analysis with somewhat increased data sample.
- ¹⁸In contrast, a recent reanalysis by Block and Cahn of σ_{tot} data including new data from the UA5 Collaboration at $\sqrt{s}=900$ GeV, indicates that cross sections probably rise somewhat slower than $\ln^2(s)$. See M. Block, in *Strong Interactions and Gauge Theories*, proceedings of the XXI Rencontre de Moriond, Les Ares, France, 1986, edited by J.

- Tran Thanh Van (Editions Frontieres, Gif-sur-Yvette, France, 1986).
- ¹⁹R. W. Ellsworth *et al.*, Phys. Rev. D **26**, 336 (1982).
- ²⁰T. Stanev and T. K. Gaisser, in *Proceedings of the Workshop on Very High Energy Cosmic Ray Interactions*, Philadelphia, 1982, edited by M. L. Cherry, K. Lande, and R. I. Steinberg (University of Pennsylvania, Philadelphia, 1982), p. 125.
- ²¹T. K. Gaisser and F. Halzen, Phys. Rev. Lett. **54**, 1754 (1985); in *First Aspen Winter Physics Conference* (Ref. 1), p. 260.
- ²²J. Linsley, in *Proceedings of the 19th International Conference on Cosmic Rays* (Ref. 17), p. 1.
- ²³R. J. Glauber and G. Matthiae, Nucl. Phys. **B21**, 135 (1970).
- ²⁴V. A. Karmanov and L. A. Kondratuk, Pis'ma Zh. Eksp. Teor. Fiz. **18**, 451 (1973) [JETP Lett. **18**, 266 (1973)].
- ²⁵P. V. Ramanamurthy *et al.*, University of Michigan Report No. HE 75-2 1975 (unpublished).